# Effect of Hot Air Aging on the Properties of Ethylene-Vinyl Acetate Copolymer and Ethylene-Acrylic Acid Copolymer Blends

**Shuangjun Chen, Jun Zhang, Jun Su**

*Department of Polymer Science and Engineering, College of Materials Science and Engineering, Nanjing University of Technology, Nanjing 210009, People's Republic of China*

Received 2 July 2008; accepted 14 October 2008
DOI 10.1002/app.29506
Published online 28 January 2009 in Wiley InterScience (www.interscience.wiley.com).

**ABSTRACT:** The aim of this investigation is to evaluate the effect of hot air aging on properties of ethylene-vinyl acetate copolymer (EVA, 14 wt % vinyl acetate units), ethylene-acrylic acid copolymer (EAA, 8 wt % acrylic acid units), and their blends. Attenuated total reflection-Fourier transform infrared spectroscopy, differential scanning calorimeter (DSC), wide angle X-ray diffraction, and mechanical tests are employed to investigate the changes of copolymer blends' structures and properties. Increase of carbonyl index derived from ATR measurements with aging time suggests the incorporation of oxygen into the polymeric chain. By DSC measurements, the enthalpy at low temperature endothermic peak ($T_{m2}$) of EAA becomes less and disappears after 8 weeks aging, but enthalpy at $T_{m2}$ of EVA is not influenced by the hot air aging and remains stable despite of the aging time. For various proportions of EAA and EVA blends, enthalpy at $T_{m2}$ decreases as the EAA proportion increases when aging time is 8 weeks; after several weeks of hot air aging, the various blends appear a same new peak just over the aging temperature 70°C which is due to the completion of crystals which are not of thermodynamic equilibrium state. Mechanical tests show that increase of crystallinity and hot air aging deterioration both have influence on the hardness, tensile strength, and elongation at break. © 2009 Wiley Periodicals, Inc. J Appl Polym Sci 112: 1166–1174, 2009

**Key words:** hot air aging; ethylene-vinyl acetate copolymer; ethylene-acrylic acid copolymer; blend; crystallization

## INTRODUCTION

Ethylene copolymers, such as ethylene-vinyl acetate copolymer (EVA) and ethylene-acrylic acid copolymer (EAA), have wide range of utilization in different industries.[1] For example, because of its wide range of properties depending on its vinyl acetate content, EVA has become one of the most useful copolymers in the transportation industry as an insulator, in the electric industry as a cable insulator, in the shoe industry used as soles, and in many other industries as an hot melt adhesive, a coating, etc.[2]

Blends of EVA are extensively used in industries because of its easy availability, processability, and excellent optical properties.[3] EVA and EAA blends were used as compatibilizers with high-density polyethylene, low-density polyethylene, and polypropylene.[4] And the blend consisting of nylon 6 and EVA compatibilized with EAA was examined to be toughened and of dramatic increase in impact strength.[5] During long-term use, the ethylene copolymers have to undergo aging or degradation like other polymeric materials due to environment conditions, especially the heat and atmospheric oxygen. The thermal or thermo-oxidative degradation of ethylene copolymers[6–11] have been widely studied. However, the hot air aging of semicrystalline polymer blend of EVA and EAA has not been investigated.

In this study, effect of hot air aging on the properties of EVA/EAA blends is investigated employing attenuated total reflection-Fourier transform infrared spectroscopy (ATR-FTIR), differential scanning calorimeter (DSC), wide angle X-ray diffraction (WAXD), and mechanical tests. ATR-FTIR is used to characterize the changes of chemical structures during the hot air aging treatment. DSC is used to find out the melting and crystallization behavior of the blend in the aging process. WAXD is used for the characterization of crystallization phase changes. And mechanical tests are performed to study the deterioration of the mechanical properties.

## EXPERIMENTAL

### Materials

EAA (Primacor3002) was supplied by Dow Chemical Company with AA content percent = 8 wt % and

*Correspondence to:* J. Zhang (zhangjun@njut.edu.cn).
Contract grant sponsor: China Postdoctoral Science Foundation; contract grant number: 20070421003.


© 2009 Wiley Periodicals, Inc.

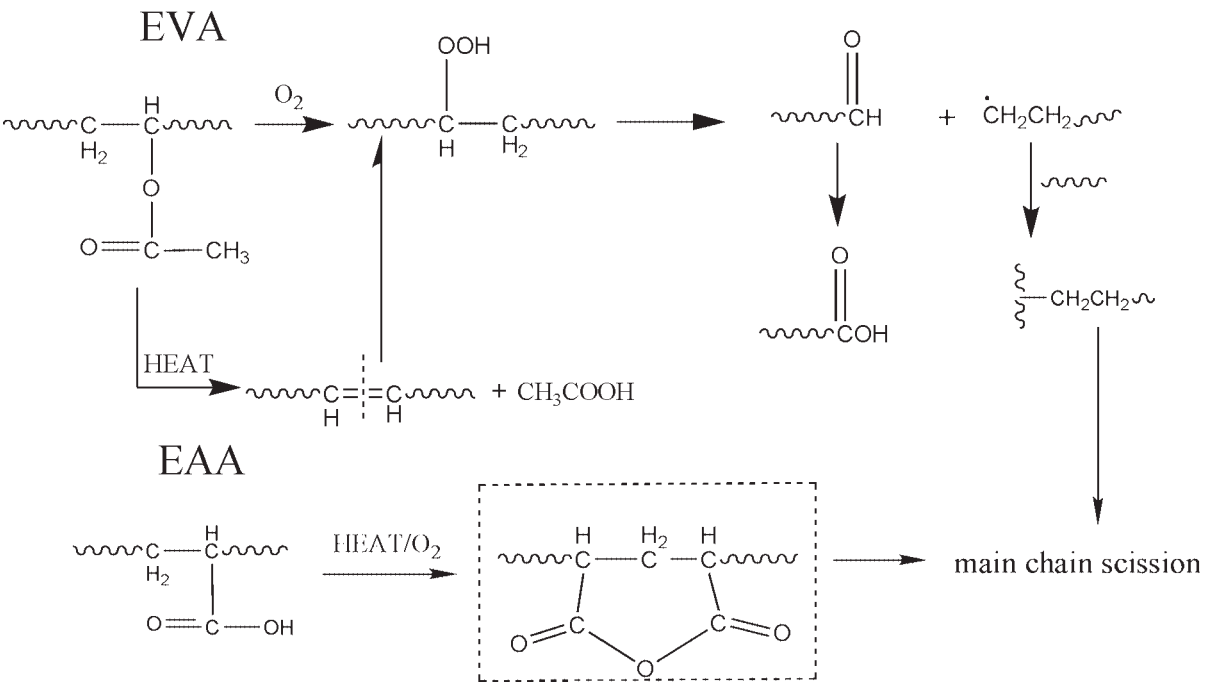


**Scheme 1** Schematic presentation of degradation mechanism of EVA and EAA.[2]

melting flow rate (MFR) = 9.8 g/10 min. EVA (14-2) was obtained from Beijing Organic Chemical Plant with vinyl acetate units (VAc) content percent = 14 wt % and MFR = 2.0 g/10 min.

### Preparation method of samples

EAA and EVA blends in various proportions of 100/0, 70/30, 50/50, 30/70, 0/100 (mass ratio) were first prepared to be aggregates by granulation from twin screw extruder, then the blends were injected to form sheets with size of 120 mm × 30 mm × 2 mm. Stamping knife was used to cut the sheet to prepare dumb-bell shape samples.

### Hot air aging

According to China National Standard GB/T 7141-92 (NEQ JIS K7212-1999), hot air aging was carried out in air at temperature 70°C, for different time (1 week, 2 weeks, 4 weeks, 6 weeks, 8 weeks).

### Characterization techniques

ATR-FTIR spectra were achieved by employing spectrometer (Bruker Vector-22) in the range from 580 to 4000 $cm^{-1}$ with 4 $cm^{-1}$ resolution.

Thermal analysis was performed on a Perkin–Elmer DSC-7C differential scanning calorimeter (DSC) under an argon atmosphere. The temperature range of scanning was from 0 to 150°C at a heating rate of 10°C/min to observe the endothermic peak of the melting transition. The crystallinity of EAA and EVA blend ($X_c$) was calculated below, as our previous work.[12,13]

$$X_c = \frac{\Delta H_f}{\Delta H_f^*} \times 100\% \quad (1)$$

where $\Delta H_f^*$ is the enthalpy of fusion of the perfect polyethylene (PE) crystal, $\Delta H_f$ is the enthalpy of fusion of the EAA/EVA blends measured in DSC. The value of $\Delta H_f^*$ for PE is 277.1 J/g in literature.[14]

To characterize the phases in some detail, WAXD was done in a Shimadzu XRD-6000 diffractometer (Cu Kα radiation, 40 kV and 30 mA). The scanning angle 2θ ranged from 5° to 50° with the scanning velocity of 4°/min. The grain size of crystallite was assigned to be $L_{hkl}$, which is the lamellar thickness in the direction perpendicular to the (*hkl*) crystal plane calculated by Scherrer Formula as reported in previous work[15]:

$$L_{hkl} = 0.89 \times \lambda/(\beta \times \cos\theta) \quad (2)$$

where λ = 1.54056 Å is wavelength of X-ray and β is half-peak width of diffraction peak.

The tensile strength and elongation at break were measured by electronic pulling tester with a crosshead speed of 50 mm/min and a gauge length of 25 mm. The test was conducted under the condition according to ISO 527-1:1993 (IDT GB/T 1040.1-2006). Shore D hardness of origin and hot air aged samples were recorded according to ISO 868:2003 (IDT GB T2411-1980).

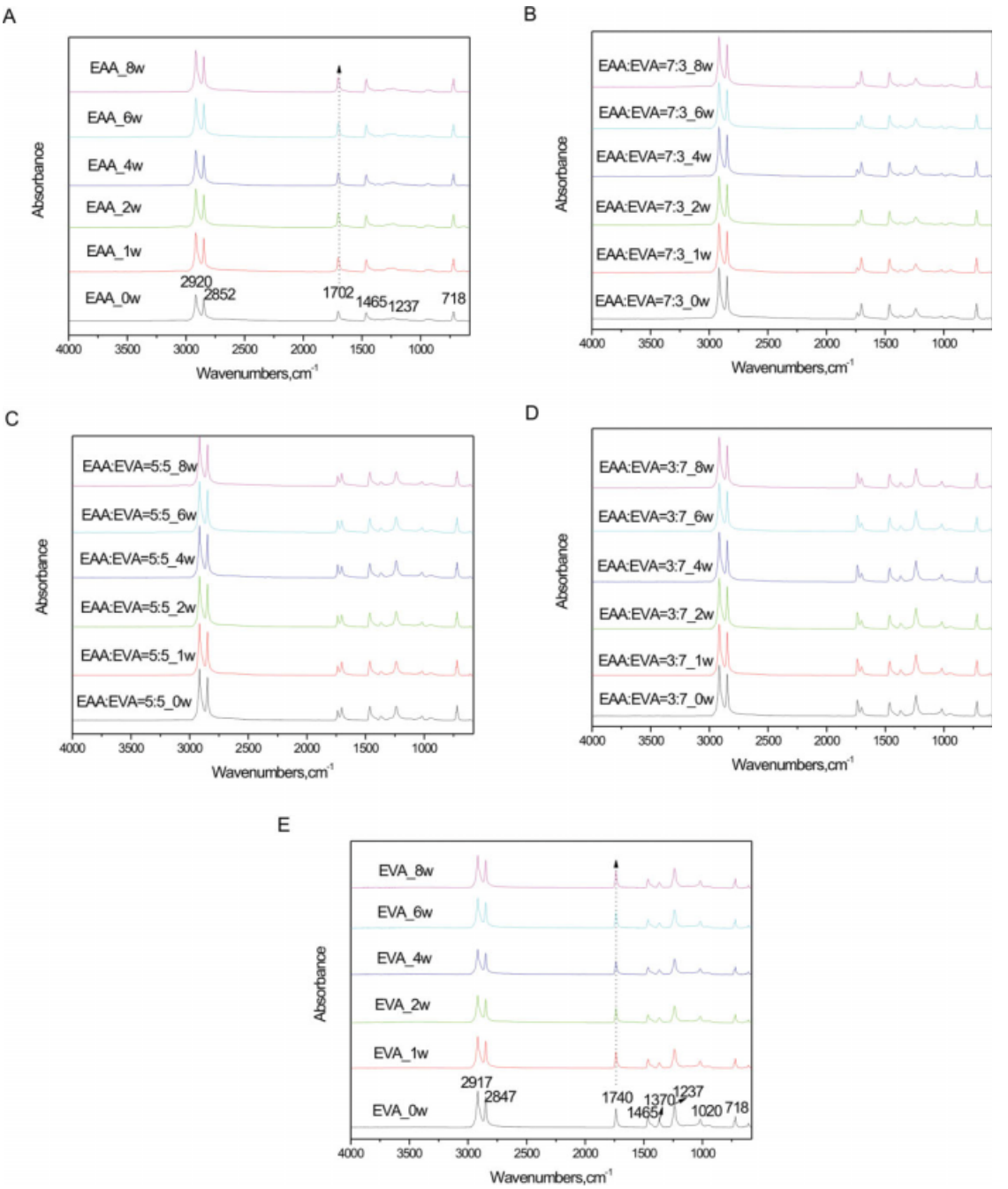


**Figure 1** ATR-FTIR spectra of various EAA/EVA blends before and after several weeks of hot air aging. [Color figure can be viewed in the online issue, which is available at www.interscience.wiley.com.]

## RESULTS AND DISCUSSION

### ATR-FTIR characterization of EAA/EVA blends

Scheme 1 presents the degradation mechanism of EVA and EAA independently. During the hot air aging process of EVA and EAA, thermo and oxidation both have effect on the properties of the copolymers. As reported, oxidative degradation of EVA produces first the ketone formation via acetaldehyde formation, and then the formation and destruction of aldehydes to form carboxylic acids. Besides, it was suggested that crosslinks via randomly distributed double bonds could possibly occur after abstraction of hydrogen in the allyl position.[2] And the last was the main chain scission, which is the degradation of the polymeric chain and finally oxidation of the carbonaceous residue.[16,17] EVA copolymers undergo a pyrolysis involving two-step decomposition: an acetate pyrolysis of the copolymer leaving a polyunsaturated linear hydrocarbon and evolving mainly acetic acid, followed by the breakdown of the hydrocarbon backbone to produce a

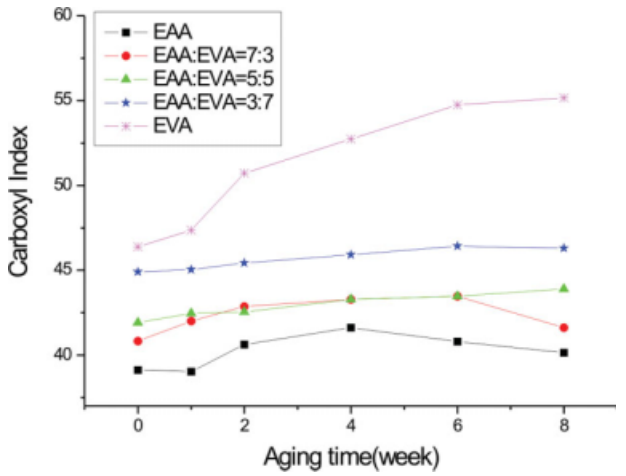


**Figure 2** Carbonyl index of various EAA/EVA blends before and after several weeks of hot air aging. [Color figure can be viewed in the online issue, which is available at www.interscience.wiley.com.]

large number of straight-chain hydrocarbon products for nonoxidative decomposition.[10] In the presence of oxygen, the followed procedure is similar to the oxidative degradation of EVA. For EAA, there are few literatures about the aging of EAA copolymers. In general, the degradation of EAA includes first the dehydration to generate poly(circular acid anhydride) and then the decomposition of poly(circular acid anhydride) at higher temperature.

Figure 1 is the ATR-FTIR spectra of EAA and EVA before and after several weeks of hot air aging. Characteristic absorption peaks of EAA and EVA are signed in Figure 1(A,E). In Figure 1(A), for ethylene segments, the characteristic absorption peaks are as follows: 2920 and 2852 $cm^{-1}$ attributed to the symmetrical and asymmetrical stretching vibration of methylene; 1465 $cm^{-1}$ attributed to deformation vibration of methylene; 1370 $cm^{-1}$ attributed to flexural vibration of methyl; 718 $cm^{-1}$ attributed to inner rocking vibration of methylene, and characteristic absorption peaks of AA groups is 1702 $cm^{-1}$ attributed to O=C—O group.[18] In Figure 1(E), the characteristic absorption peaks of ethylene segments are similar with those in Figure 1(A). Characteristic absorption peaks of VAc groups are as follows: 1740 $cm^{-1}$ attributed to stretching vibration of C=O band; 1237 $cm^{-1}$ attributed to asymmetrical stretching vibration of C—O band; 1020 $cm^{-1}$ attributed to symmetric stretching vibration of C—O—C band.[2] In Figure 1(B–D), besides the absorption peaks of ethylene segments, peaks at 1702 $cm^{-1}$ of EAA and 1740 $cm^{-1}$ of EVA have different strengths due to the different mass ratio of EAA and EVA. As aging time increases from 1 week to 8 weeks, both thermo and oxidation have effect on the degradation of the blends.

According to Scheme 1, the main sequence of hot air aging on the blends is the loss or formation of O=C group, the course of hot air aging is followed by using a carbonyl index (CI) derived from ATR-FTIR measurement.[19] In this study, the CI is defined as the ratio of the peak area between 1850 and 1500 $cm^{-1}$ ($A_{1800-1500}$) and the absorption of the peak at 1463 $cm^{-1}$ ($A_{1463}$):

$$CI = A_{1800-1500}/A_{1463}$$

Figure 2 shows the CI derived from ATR-FTIR figures for the various EAA/EVA blends. Generally the introduction of polar groups reduces the thermal stability, and more polar groups induce less thermal stability, so for EAA with AA content 8 wt % the CI has not very obvious change while for EVA with VAc content 14 wt %, the CI has increased a lot as the aging time increases. It is also observed in Figure 2 that the CIs of various blends of EAA/EVA have the same tendency that the CI increases as the aging time increases. This means that in the hot air aging process, the incorporation of oxygen into the polymeric chain is more competitive than the loss of acetate.

## Hot air aging on crystallization behavior of EAA/EVA blends

The crystallization behavior of random copolymers undergoes two types of fractionation: The first is thermodynamic in nature and takes place at high crystallization temperature or upon slow cooling from the melt. This process leads to formation of lamellar crystals and involves only those sequences of regular units that are sufficiently long to form ordered domains with the thickness dictated by the actual undercooling.[20] The other is of a kinetic nature and takes place at relatively low temperature and involves successive clustering of residual regular sequences. In the early stages of this slow process, metastable domains with an intermediate level of order are formed in which a fraction of defective units might be included into the loose lattice.[21]

Figure 3 is the DSC curves of the various EAA/EVA blends before and after 8 weeks of hot air aging. Because the original samples have various thermal histories, their DSC curves are of multiple peaks which are not significative to discuss. We use $T_{m1}$ for the new formed higher temperature endothermic peak of EAA component after 1 week aging and $T'_{m1}$ for the new formed higher temperature endothermic peak of EVA after 1 week aging; these peaks or shoulders are attributed to the primary crystallization; because the low temperature crystallization of EVA and EAA blends are compatible, only one $T_{m2}$ is used to represent the low temperature endothermic peak; after several weeks of hot air

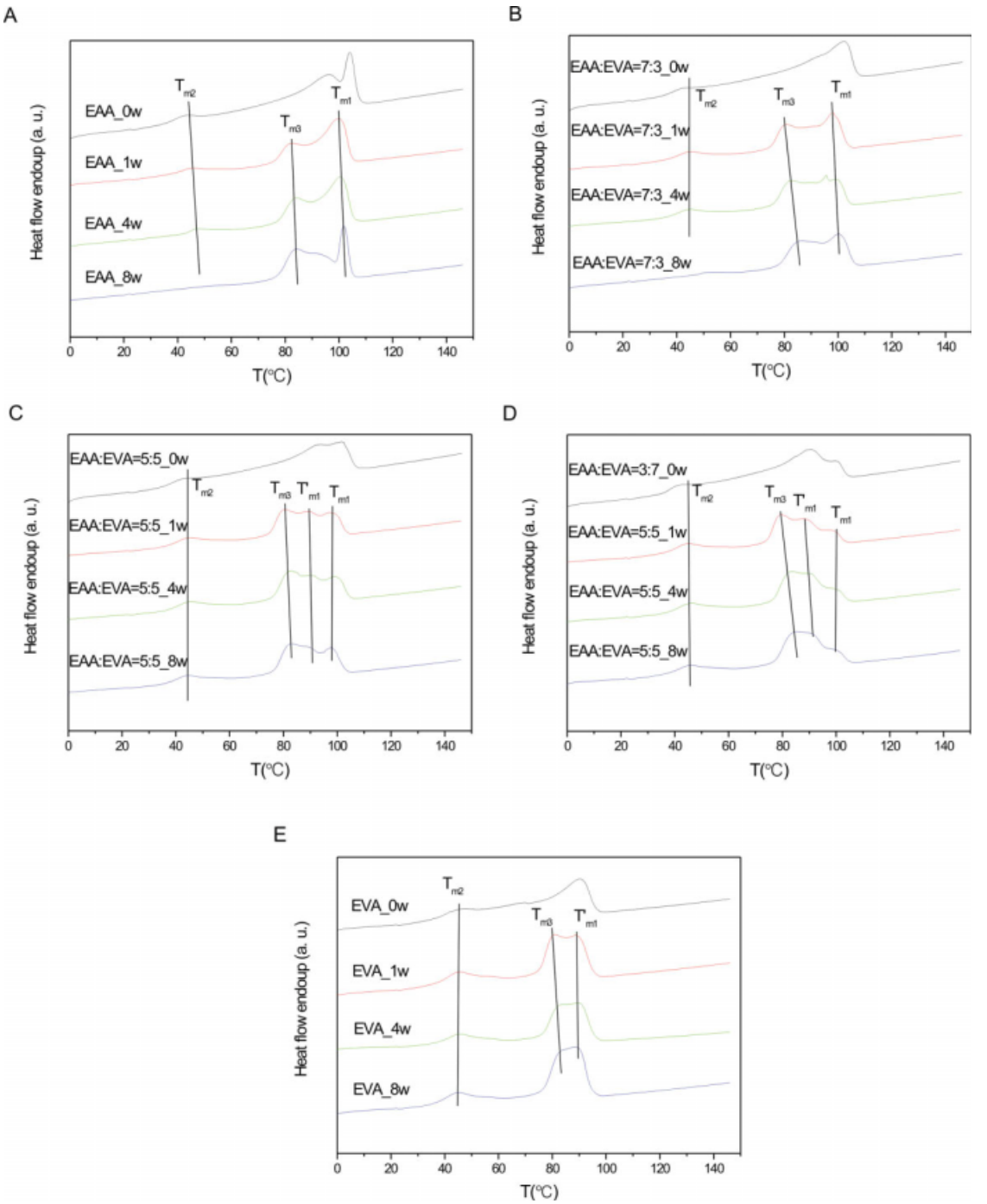


**Figure 3** DSC curves of the various EAA/EVA blends as aging time increase: (A) EAA; (B) EAA : EVA = 7 : 3; (C) EAA : EVA = 5 : 5; (D) EAA : EVA = 3 : 7; (E) EVA. [Color figure can be viewed in the online issue, which is available at www.interscience.wiley.com.]

aging, the various blends appear a same new peak just over the aging temperature 70°C which is represented by $T_{m3}$. The data of melting peaks derived from DSC curves are listed in Table I and degree of crystallinity in Table II in detail.

Comparatively, it can be observed that during the same thermal history, EAA with longer sequence-length of ethylene chain need more time to thermodynamic equilibrium state than EVA.[22] For various proportions of EAA and EVA blend, there are multiple endothermic peaks and shoulders, attributed to EAA and EVA, respectively.[23] For EAA in Figure 3(A) and EVA in Figure 3(E) independently, when hot air aging time increases from 1 week, 4 week to 8week, $T_{m1}$ increases from 99.8, 100.5 to 101.7°C and $T'_{m1}$ increases from 89.0, 89.4 to 89.7°C as shown in

**TABLE I**
**Melting Peaks of Various EAA/EVA Blends as Aging Time Increases**

| Samples | Aging time (weeks) | $T_{m1}/T'_{m1}$ (°C) | $T_{m2}$ (°C) | $T_{m3}$ (°C) |
|---|---|---|---|---|
| EAA | 0 | – | 44.4 | – |
| | 1 | – | 45.6 | 82.5 |
| | 4 | 100.5 | 47.8 | 84.2 |
| | 8 | 101.7 | – | 83.9 |
| EAA : EVA = 7 : 3 | 0 | – | 44.7 | – |
| | 1 | 97.6 – | 44.6 | 80.6 |
| | 4 | 99.2 – | 44.3 | 82.4 |
| | 8 | 100.1 – | – | 85.5 |
| EAA : EVA = 5 : 5 | 0 | – | 44.4 | – |
| | 1 | 98.3 89.6 | 44.4 | 80.5 |
| | 4 | 98.9 89.8 | 45.3 | 82.3 |
| | 8 | 98.0 89.2 | 44.4 | 82.6 |
| EAA : EVA = 3 : 7 | 0 | – | 45.0 | – |
| | 1 | 100.1 87.9 | 45.3 | 79.2 |
| | 4 | 99.8 89.8 | 45.4 | 82.6 |
| | 8 | 99.8 90.9 | 45.6 | 84.2 |
| EVA | 0 | – | 45.0 | – |
| | 1 | 89.0 | 45.0 | 80.5 |
| | 4 | 89.4 | 44.9 | 82.3 |
| | 8 | 89.7 | 44.7 | 83.0 |

Table I. However, for the EAA/EVA blends in Figure 3(D,E), when hot air aging time increases from 1 week, 4 weeks to 8 weeks, $T_{m1}$ decreases from 98.3, 98.7 to 98.0°C and $T'_{m1}$ has also a little decrease from 89.6, 89.8, and 89.2°C. The $T_{m1}$ and $T'_{m1}$ are both contributed to primary crystallization which has no time to obtain thermodynamic equilibrium state. When the hot air aging time at 70°C increases, very small parts of chains among primary crystal are melted and reorganized, so that during 8 weeks of hot aging, $T_{m1}$ and $T'_{m1}$ become close to some content, because the aging process makes the chains with near sequence length reorganize.

Before hot air aging, the low temperature endothermic peaks ($T_{m2}$) of various EAA/EVA blends at about 44.5°C are attributed to the secondary crystallization which did not crystallize perfectly.[24,25] In Figure 3(A,E), as aging time increases, it is interesting to observe that enthalpy at $T_{m2}$ of EAA becomes less and disappears after 8 weeks aging, but enthalpy at $T_{m2}$ of EVA is not influenced by the hot air aging and remains at about 44.5°C despite of the aging time. For various proportions of EAA and EVA blend, enthalpy at $T_{m2}$ deceases as the EAA proportion increased when aging time is 8 weeks. Considering the EAA with 8 wt % AA has longer sequence-length than EVA with 14 wt % VAc, this phenomenon indicates that the ethylene chains with longer sequence in EAA have the ability to rearrange to the crystal lattice formed during the annealing process at 70°C, but the ethylene chains with shorter sequence EVA are unable to rearrange into the later formed crystal.[20]

In Table I and Figure 3, $T_{m3}$ is just over the aging temperature 70°C. And for various EAA/EVA blends after several weeks of hot air aging, there are all one $T_{m3}$ which is just over the aging temperature 70°C and as aging time increases, the peaks increase about 1–2°C. For example, in Figure 3(D), as aging time is 1 week, the peak is at 79.2°C, and then 82.6, 84.0°C when the aging time is 4 weeks and 8 weeks. In Figure 3(E) for the EVA copolymer, $T_{m3}$ at 80.5°C increases to the one at 83.0°C after aging for 8 weeks at 70°C. The melting behavior is consistent with the hypothesis of Marand and collaborators[26] that the slow secondary crystallization at low temperatures leads to crystals with very poor stability. When aging at 70°C for some time, reorganization of

**TABLE II**
**Degree of Crystallinity of Various EAA/EVA Blends as Aging Time Increases**

| Samples | Degree of crystallinity (%) | | | |
|---|---|---|---|---|
| | Aging time 0 week | Aging time 1 week | Aging time 4 weeks | Aging time 8 weeks |
| EAA | 29.23 | 32.97 | 31.88 | 31.02 |
| EAA : EVA = 7 : 3 | 27.12 | 32.96 | 32.96 | 28.39 |
| EAA : EVA = 5 : 5 | 25.36 | 31.08 | 30.59 | 31.37 |
| EAA : EVA = 3 : 7 | 25.40 | 29.52 | 30.36 | 30.01 |
| EVA | 22.31 | 29.56 | 28.90 | 29.46 |

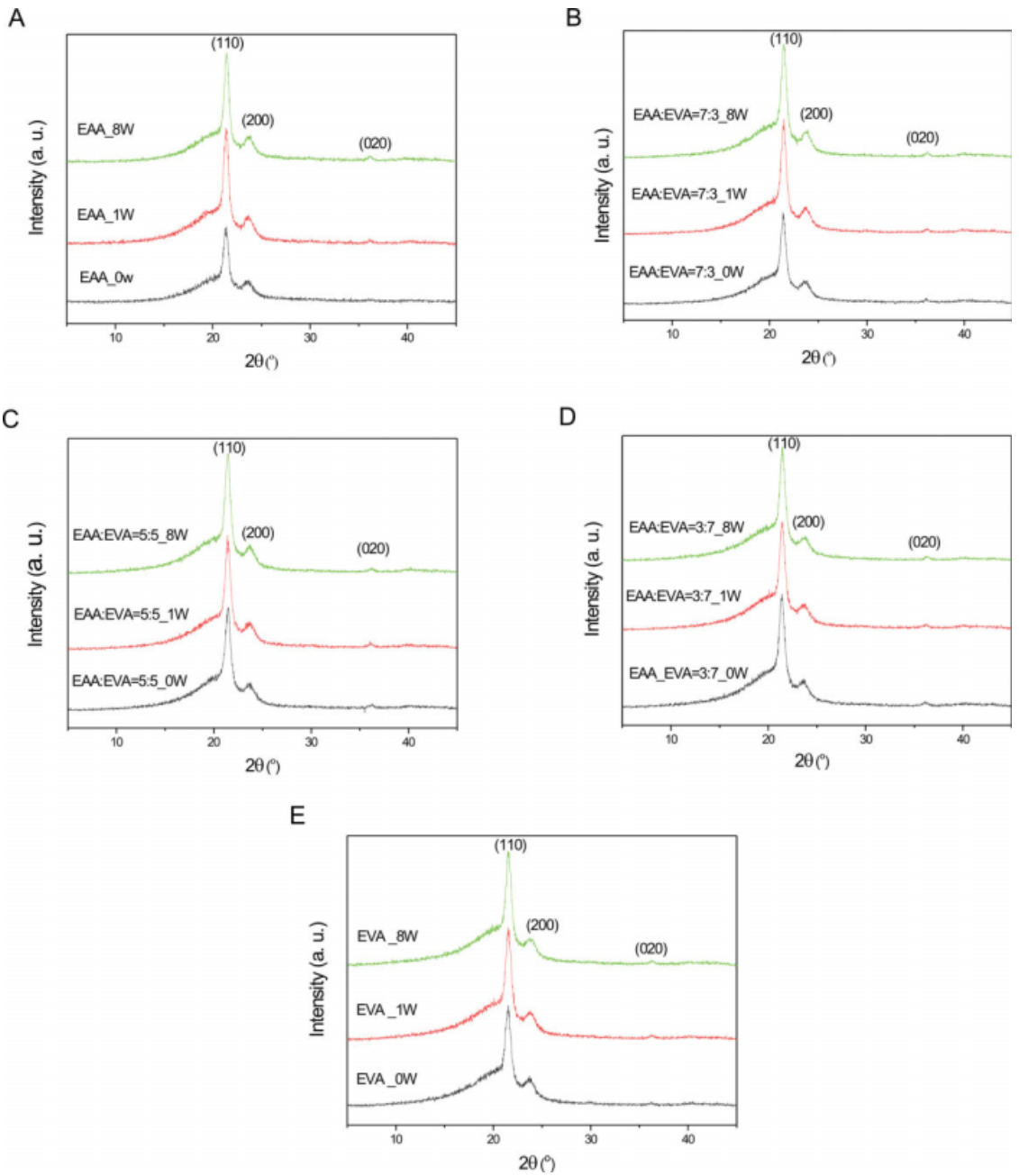


**Figure 4** WAXD patterns of the various EAA/EVA blends as aging time increase: (A) EAA; (B) EAA : EVA = 7 : 3; (C) EAA : EVA = 5 : 5; (D) EAA : EVA = 3 : 7; (E) EVA. [Color figure can be viewed in the online issue, which is available at www.interscience.wiley.com.]

polymer chains in the interphase state or amorphous state happens to form a new ordered domain which is promoted by the hot air aging at 70°C. What is more, the degree of crystallinity of various EAA/EVA blends is enhanced a lot when the aging time is 1 week, and as the time increases, the values almost keep stable which are presented in detail in Table II. For EAA/EVA blend with proportion of 5 : 5, degree of crystallinity increases from 25.36 to 31.08% when aging time is 1 week, and remain almost same of 31.37% when aging time is 8 weeks.

Figure 4 shows the WAXD patterns of EVA, EAA, and their blends before and after 8 weeks of hot air aging. It has been reported that besides the stable orthorhombic phase (from the primary crystallization), a secondary crystallization phase (monoclinic) also appears in EVA copolymers under normal crystallization conditions (i.e., quenching, aircooling, or solution-crystallized).[27,28] In general, a two-crystal model, say, e.g., longer ethylene sequences tend to crystallize into orthorhombic phase and shorter ones tend to crystallize into monoclinic phase, is widely accepted for the

**TABLE III**
**Grain Size $L_{hkl}$ of (110) Crystal Plane of Various EAA/EVA Blends as Aging Time Increases**

| Samples | $L_{hkl}$ (Å) of (110) crystal plane | | |
|---|---|---|---|
| | Aging time 0 week | Aging time 1 week | Aging time 8 weeks |
| EAA | 108 | 115 | 126 |
| EAA : EVA = 7 : 3 | 105 | 110 | 108 |
| EAA : EVA = 5 : 5 | 101 | 107 | 106 |
| EAA : EVA = 3 : 7 | 100 | 105 | 105 |
| EVA | 96 | 97 | 100 |

long-branch copolymers.[29] Monoclinic phase often exists in the shorter ethylene sequences with more polar groups like VAc or AA. Besides the monoclinic, recently the secondary crystallization phase was attributed to third crystalline phase, named short time relaxation part of orthorhombic phase (SOCP) which was detected by solid-state NMR and DSC. Such a third crystalline phase forms during room-temperature aging and melts at the temperature somewhat higher than room temperature on heating. However, no well-resolved reflections from monoclinic phase and SOCP phase were detected by WAXD at room temperature.[30,31] This is conformed by our experiment results of WAXD as shown in Figure 4. Three perceptible diffractive peaks around 21.5°, 23.7°, and 36.3° are relative to typical (110), (200), and (020) crystallographic planes of orthorhombic phase, respectively. Before [Fig. 4(A)] and after [Fig. 4(B)] 8 weeks of hot air aging, there are no obvious changes in the diffractive peaks. On the other hand, in Table III, the grain size $L_{hkl}$ (Å) of (110) crystal plane of various EAA/EVA blends is listed. It is observed that the $L_{hkl}$ of (110) crystal plane has the same tendency to increase with the hot air aging time, which indicates the completion of secondary crystallization. Another point is that as the EAA content of blends increases, the $L_{hkl}$ of (110) crystal plane increases which is consistent with the above observation.

### Hot air aging on the mechanical properties of EAA/EVA blends

Variation of the mechanical properties of the samples with hot air aging time is shown in Figure 5. On the one hand, the hot air aging will reduce the mechanical properties of EAA/EVA blends; on the other hand, hot air aging of EAA/EVA blends will increase the degree of crystallinity which will enhance the mechanical properties. As mentioned, the degree of crystallinity of various EAA/EVA blends is enhanced a lot when the aging time is 1 week, as the time increases more than 1 week, the values almost keep stable. Accordingly for pure EAA in Figure 5(A), it is found that the Shore D hardness firstly decreases due to aging damage, and then is enhanced a lot when the aging time is 2 weeks, and as the time is 4 weeks or 8 weeks, the Shore D hardness almost keeps stable. For other EAA/EVA blends, the two influence factors are

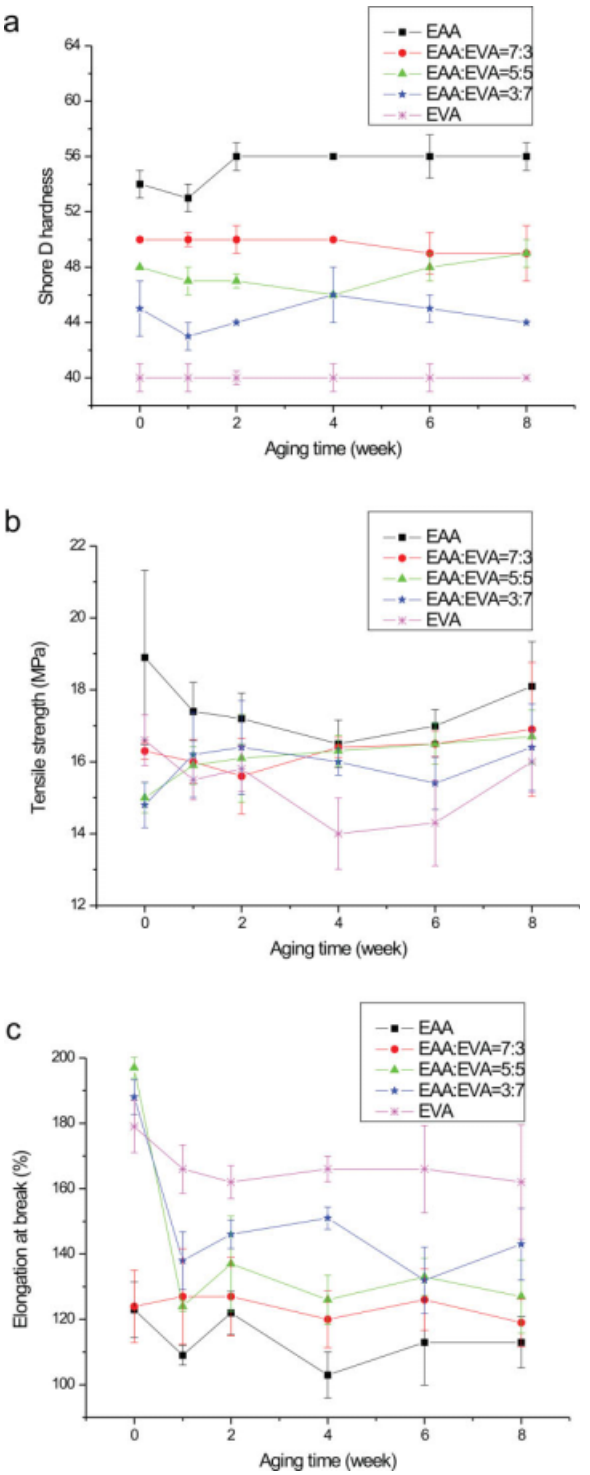


**Figure 5** Mechanical properties of the various EAA/EVA blends as aging time increase: (A) Shore D hardness versus aging time from 0 to 8 weeks; (B) tensile strength versus aging time from 0 to 8 weeks; (C) elongation at break versus aging time from 0 to 8 weeks. [Color figure can be viewed in the online issue, which is available at www.interscience.wiley.com.]

competitive so that the hardness appears no obvious change law. In Figure 5(B), the tensile strengths of pure EAA and pure EVA sample decrease as aging time increases due to the deterioration but the EAA/EVA blends have no obvious changes in tensile strength because the primary crystallite did not be influenced so much. In Figure 5(C), the elongation at break values of various EAA/EVA blends decrease when the aging time is 1 week, however, as the time increase more to 4 weeks or 8 weeks, the values almost keep stable. What is more, the polar content will have much effect on the mechanical properties, including hardness, tensile strength in Figure 5(B), and elongation at break in Figure 5(C). Because the AA content of EAA is 8 wt % while the VAc content of EVA is 14 wt %, it can be observed that as the proportion of EAA increases, the sample has higher hardness, higher tensile strength with lower elongation at break attributed to higher crystallinity.[32]

## CONCLUSIONS

Data presented here show that increase of CI derived from ATR-FTIR measurements with aging time suggests the incorporation of oxygen into the polymeric chain. In DSC data, the enthalpy at $T_{m2}$ of pure EAA at about 44.5°C attributed to the secondary crystallization disappears after 8 weeks aging, but enthalpy at $T_{m2}$ of pure EVA is not influenced a lot by the hot air aging, and as the EVA contents increase, the influence of aging on the low temperature endotherm of EVA and EAA blends become less; after several weeks of hot air aging, the various blends appear a same new peak just over the aging temperature 70°C which is due to the completion of crystals with very poor stability. From WAXD patterns, there are no obvious changes in the diffractive peaks, but $L_{hkl}$ of (110) crystal plane has the same tendency to increase with the hot air aging time. And mechanical tests show that degree of crystallinity and hot air aging deterioration both have influence on Shore D hardness, tensile strength, and elongation at break.

## References


1. Allen, N. S.; Edge, M.; Rodriguez, M.; Liauw, C. M.; Fontan, E. Polym Degrad Stab 2000, 71, 1.
2. Copuroglu, M.; Sen, M. Polym Adv Technol 2004, 15, 393.
3. Siddaramaiah; Bhattacharya, A. K.; Nando, G. B. J Appl Polym Sci 2005, 98, 1947.
4. McEvoy, R. L.; Krause, S. Macromolecules 1996, 29, 4258.
5. Wang, X. D.; Li, H. Q.; Ruckenstein, E. Polymer 2001, 42, 9211.
6. Allen, N. S.; Edge, M.; Rodriguez, M.; Liauw, C. M.; Fontan, E. Polym Degrad Stab 2000, 68, 363.
7. Giurginca, M.; Popa, L.; Zaharescu, T. Polym Degrad Stab 2003, 82, 463.
8. Marcilla, A.; Gomez, A.; Menargues, S. Polym Degrad Stab 2005, 89, 454.
9. Marcilla, A.; Gomez, A.; Menargues, S. Polym Degrad Stab 2005, 89, 145.
10. Marcilla, A.; Gomez, A.; Menargues, S. J Anal Appl Pyrolysis 2005, 74, 224.
11. Mares, G. Polym Degrad Stab 1995, 50, 29.
12. Gu, M. H.; Zhang, J.; Wang, X. L. J Appl Polym Sci 2006, 102, 3714.
13. Tao, H. J.; Zhang, J.; Wang, X. L.; Gao, J. L. J Polym Sci Part B: Polym Phys 2007, 45, 153.
14. Brandrup, J.; Immergut, E. H. Polymer Handbook, 3rd ed.; Wiley: New York 1999; p 736.
15. Suryanarayana, C.; Grant, N. M. X-Ray Diffraction: A Practical Approach; Plenum Press: New York, 1998.
16. Marcilla, A.; Gomez-Siurana, A.; Menargues, S. J Therm Anal Calorim 2007, 87, 519.
17. Marcilla, A.; Gomez-Siurana, A.; Menargues, S.; Ruiz-Femenia, R.; Garcia-Quesada, J. C. J Anal Appl Pyrolysis 2006, 76, 138.
18. Klemchuk, P.; Ezrin, M.; Lavigne, G.; Holley, W.; Galica, J.; Agro, S. Polym Degrad Stab 1997, 55, 347.
19. Bikiaris, D.; Prinos, J.; Panayiotou, C. Polym Degrad Stab 1997, 56, 1.
20. Akpalu, Y.; Kielhorn, L.; Hsiao, B. S.; Stein, R. S.; Russell, T. P.; van Egmond, J.; Muthukumar, M. Macromolecules 1999, 32, 765.
21. Azzurri, F.; Alfonso, G. C.; Gomez, M. A.; Marti, M. C.; Ellis, G.; Marco, C. Macromolecules 2004, 37, 3755.
22. Hu, W. B.; Mathot, V. B. F. Macromolecules 2004, 37, 673.
23. Velikov, V.; Marand, H. J Therm Anal 1997, 49, 375.
24. Cho, T. Y.; Shin, E. J.; Jeong, W.; Heck, B.; Graf, R.; Strobl, G.; Spiess, H. W.; Yoon, D. Y. Macromol Rapid Commun 2006, 27, 322.
25. Rastogi, S.; Terry, A. E. Adv Polym Sci 2005, 180, 161.
26. Alizadeh, A.; Richardson, L.; Xu, J.; McCartney, S.; Marand, H.; Cheung, Y. W.; Chum, S. Macromolecules 1999, 32, 6221.
27. Zhang, Q. J.; Lin, W. X.; Yang, G.; Chen, Q. J Polym Sci Part B Polym Phys 2002, 40, 2199.
28. Su, Z. Q.; Zhao, Y.; Xu, Y. H.; Zhang, X. Q.; Zhu, S. N.; Wang, D. J.; Wu, J. G.; Han, C. C.; Xu, D. F. Macromolecules 2004, 37, 3249.
29. Hu, W. G.; Sirota, E. B. Macromolecules 2003, 36, 5144.
30. Wang, L. Y.; Fang, P. F.; Ye, C. H.; Feng, J. W. J Polym Sci Part B Polym Phys 2006, 44, 2864.
31. Wang, L. Y.; Zhao, X. Z.; Feng, J. W. J Polym Sci Part B Polym Phys 2006, 44, 1714.
32. Kundu, P. P.; Choudhury, R. N. P.; Tripathy, D. K. J Appl Polym Sci 1999, 71, 551.